Strain engineering to control the magnetic and magnetotransport properties of $La_{0.67}Sr_{0.33}MnO_3$ thin films

F. Yang[1], N. Kemik[1], M.D. Biegalski[2], H.M. Christen[2], E. Arenholz[3], Y. Takamura[1]

[1]*Department of Chemical Engineering and Materials Science, University of California–Davis, Davis, California 95616, USA*
[2]*Center for Nanophase Materials Science, Oak Ridge National Laboratory, Oak Ridge, Tennessee 37831, USA*
[3]*Advanced Light Source, Lawrence Berkeley National Laboratory, Berkeley, California 94720, USA*

This work studies the control of the magnetic and magnetotransport properties of $La_{0.67}Sr_{0.33}MnO_3$ thin films through strain engineering. The strain state is characterized by the tetragonal distortion (c/a ratio), which can be varied continuously between a compressive strain of 1.005 to a tensile strain of 0.952 by changing the type of substrate, the growth rate, and the presence of an underlying $La_{0.67}Sr_{0.33}FeO_3$ buffer layer. Increasing tensile tetragonal distortion of the $La_{0.67}Sr_{0.33}MnO_3$ thin film decreases the saturation magnetization, changes the temperature dependence of the resistivity and magnetoresistance, and increases the resistivity by several orders of magnitude.

The perovskite oxides have been widely investigated in recent years since they possess various important physical properties such as ferromagnetism, superconductivity, and ferroelectricity.[1] In particular, $La_{0.67}Sr_{0.33}MnO_3$ (LSMO) is an attractive candidate for spintronic devices[2,3] because it displays colossal magnetoresistance (CMR) and half-metallicity, and possesses a Curie temperature, T_C above room temperature ($\sim$ 360 K).[4,5] In this material, the T_C marks the transition between the ferromagnetic (FM)/ metallic and the paramagnetic (PM)/ insulating states, as well as the peak in the CMR. This correlation between the electrical and magnetic properties is explained by the double-exchange mechanism[6,7] which involves the hopping of electrons between Mn^{3+} and Mn^{4+} ions with parallel spin through a bridging O^{2-} ion. Due to the strong interactions between the charge and orbital degrees of freedom, these properties can be manipulated by a number of different parameters, including external pressure[8], oxygen stoichiometry[9], and the doping level.[10,11]

With thin films, the epitaxial strain imposed from the underlying substrate provides an additional tuning parameter for the functional properties. It has been shown that coherently strained LSMO thin films can be grown on a wide range of different single crystal oxide substrates and that the resulting strain dramatically impacts the magnetic and magnetotransport properties of the thin films.[12-16] The strain state can be characterized by the tetragonal distortion, defined as the c/a ratio, where the in-plane lattice parameter of the film, a, is dictated by the lattice parameter of the substrate, and the out-of-plane lattice parameter, c, is allowed to respond accordingly. For example, Kwon *et al.* reported that an in-plane

easy magnetization direction is observed in tensile-strained films (c/a ratio < 1) grown on (001)-oriented $SrTiO_3$ (STO) substrates, while compressively strained films (c/a ratio > 1) grown on (001)-oriented $LaAlO_3$ (LAO) substrates exhibit an out-of-plane easy axis.[12] Furthermore, it has been shown that the magnitude of this tetragonal distortion depends on the crystallographic orientation of the film and the substrate. [13,14,17] Fully strained LSMO films grown on (110)-oriented substrates show enhanced electrical and magnetic properties due to the reduced tetragonal distortion relative to the films grown on (001)-oriented substrates.

Previously, Takamura *et al*. [15] showed that a dramatic change in the properties of LSMO films occurred as the c/a ratio decreased from 0.984 to 0.962. However, the strain states were limited to discrete values corresponding to the lattice parameters of the commercially available single crystal oxide substrates, STO and $DyScO_3$, respectively, therefore intermediate strain states were not available. One alternative involves using piezoelectric substrates such as $Pb(Mg_{1/3}Nb_{2/3})_{0.72}Ti_{0.28}O_3$, which allow for the dynamic modulation of the strain by varying the applied electric field.[16] However, the crystalline quality of the LSMO films grown on these piezoelectric substrates suffers due to the large lattice mismatch and the rhombohedral structure of the substrate. Furthermore, the brittleness of the substrates limits the practical range of strain that can be attained. In this work, we demonstrate the ability to control the epitaxial strain of LSMO thin films continuously over a large range through the choice of substrate, the growth rate, and the presence of an underlying $La_{0.7}Sr_{0.3}FeO_3$ (LSFO) buffer layer.

Bulk LSMO has a rhombohedral perovskite structure which can be approximated as

pseudocubic with a lattice parameter of 3.873 Å. The lattice mismatch ranges from -0.26% for cubic $(LaAlO_3)_{0.3}(Sr_2AlTaO_6)_{0.7}$ (LSAT) substrates to +2.44/2.59 % for orthorhombic $GdScO_3$ (GSO) substrates, relative to the substrate [10] and [001] directions, respectively. Bulk LSFO has an orthorhombic perovskite structure with lattice parameters a=5.50 Å, b=5.54 Å, and c=7.85 Å.[18] The lattice mismatch for LSFO varies from -1.37/-0.91% on LSAT to 1.71/1.11% on GSO substrates. A constant La/Sr ratio between the LSMO and LSFO films prevents Sr interdiffusion at the LSFO/LSMO interface. In all cases, the LSMO thin film grows with a pseudocubic (001) orientation.

The epitaxial LSMO and LSFO thin films were grown by pulsed laser deposition (PLD) using a 248 nm KrF laser operating at a frequency of 10 Hz and an energy density of ~ 1.2 J/cm^2. During the deposition, the substrate temperature was held at 700 °C and the oxygen pressure was 200 mTorr. The substrates were chosen between (001)-oriented LSAT and STO substrates and (110)-oriented GSO substrates. After the deposition, the samples were cooled in an oxygen pressure of ~ 300 Torr to obtain the proper stoichiometry of the films. Reflection high energy electron diffraction (RHEED) was used to monitor the growth rate and to control the film thickness. The crystallinity and strain state of the films were determined using high-resolution x-ray diffraction (XRD) and reciprocal space maps taken on a Bruker D8 Discover four-circle diffraction system. Magnetotransport properties were measured using a Physical Properties Measurement System using the van der Pauw geometry with a

magnetic field (Ha) applied in the plane of the film. X-ray magnetic circular dichroism (XMCD) experiments were performed at beamline 6.3.1 of the Advanced Light Source to study the surface magnetic properties with element specificity.[19] The x-rays were incident upon the sample with a 30° angle relative to the sample surface and Ha was applied parallel to the x-ray beam direction. The XMCD was calculated as the difference of two x-ray absorption spectra taken with Ha parallel/anti-parallel to the helicity of the x-rays.

X-ray diffraction θ-2θ scans (not shown) of the out-of-plane direction showed nice thickness fringes for all the samples indicating smooth surfaces and interfaces. By fitting the intensity oscillations around the Bragg peak, the film thicknesses and out-of-plane lattice parameters, c, were confirmed. Reciprocal space maps of the asymmetric 103 reflection of pseudocubic LSMO and the 332 reflection of orthorhombic LSFO were used determine the degree of coherency to the underlying substrate and the in-plane lattice parameter, a. Table I lists the structural parameters for the LSMO layer in single layer and bilayer films grown on various substrates. A fully strained film assumes the same in-plane lattice parameter as the substrate while the out-of-plane lattice parameter is free to contract or expand, therefore becoming tetragonally distorted. A fully relaxed film retains its bulk lattice parameters with c/a ratio ~ 1 for pseudocubic LSMO, and a partially relaxed film lies somewhere in between. The amount of tetragonal distortion affects the size and shape of the MnO_6 octahedral, which forms the basis of the perovskite structure and dictates its properties.

Table I: Summary of the structural and magnetic properties of the LSMO layer in single layer and bilayer films grown on various substrates.

| Sample	Thin Film Thickness (nm)	c (Å)	a (Å)	c/a	Coherency to substrate	Tc (K)	MR at Tc (%)	Maximum XMCD at 80K (arb. units)	Hc at 80K Ha∥<100> (mT)
LSMO on LSAT	40	3.897	3.879	1.005	Fully strained	345	32	0.25	1
LSMO on GSO	40	3.846	3.897	0.987	Partially relaxed	335	32	0.23 (30 K)	39 (30 K)
LSFO/LSMO on STO	30/10	3.851	3.905	0.986	Fully strained	295	32	0.20	3
LSFO/LSMO on LSAT	30/10	3.845	3.912	0.983	Partially relaxed	285	40	0.20	9
LSFO/LSMO on GSO	30/10	3.829	3.939	0.972	Partially relaxed	250	48	0.15	24
LSMO on DSO[a]	35	3.796	3.946	0.962	Fully strained	~200	~45	0.02 (30 K)	113.6 (30K)
LSMO on GSO[a]	35	3.785	3.976	0.952	Fully strained[b]	~200	~45	0.06 (30 K)	88.0 (30 K)

[a] Ref. 15
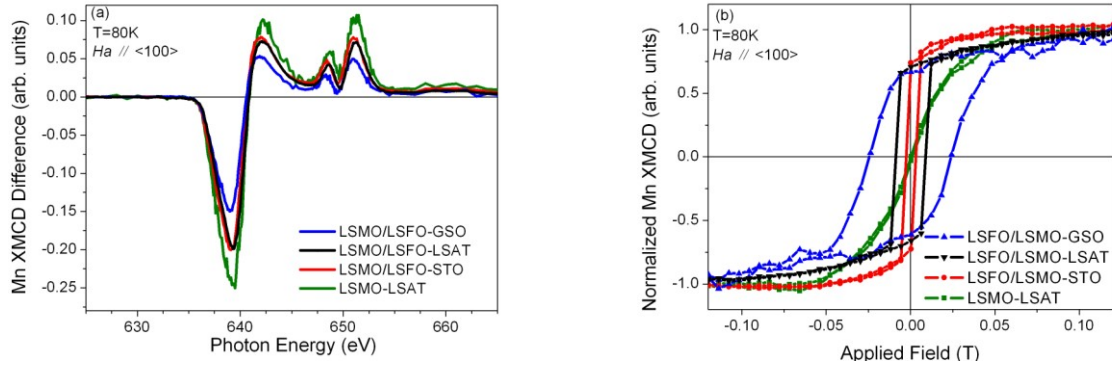
Fig.1. (a) Mn XMCD spectra and (b) Mn hysteresis loops measured at 80K for LSMO layers under varying strain states with *Ha* applied parallel to the <100> pseudocubic LSMO direction.

The XRD results show that in general, the LSFO buffer layers are unable to support as large of strain as LSMO thin films, and thus they partially relax for a lattice mismatch greater than ~ +/- 1%, i.e. on LSAT and GSO substrates. The LSMO layer grows fully strained to the underlying LSFO buffer layer, therefore, assuming *c/a* ratios that differ from the LSMO film grown directly LSAT or GSO substrates. In contrast, both LSFO and LSMO thin films are fully strained on STO substrates, and the LSMO strain state is unchanged compared to a single LSMO layer. Due to the large lattice mismatch between the LSMO film and the GSO substrate, fully strained and partially relaxed LSMO films with different *c/a* ratio are grown by changing the growth rate. In PLD, the growth rate can be controlled by varying the laser energy density, the pulse repetition rate, the target-to-substrate distance, and the ambient pressure. The growth rates are 1.3-1.7nm/min and 3.5nm/min[15] for the partially relaxed and fully strained LSMO films grown on GSO substrates respectively. We postulate that with a fast growth rate, the strain within the LSMO thin film builds up so quickly that the LSMO does not have enough time to relax, which results in a fully strained film. It should be noted that the fully strained film on GSO has reduced crystalline quality compared to the films grown on other substrates, and likely possesses a partially relaxed surface layer.[15] Therefore, we find that the epitaxial strain of LSMO film can be tuned continuously from a slight compressive strain with a *c/a* ratio of 1.005 to a large tensile strain with a *c/a* ratio of 0.952, by the choice of substrate, the growth rate, and the presence of a LSFO buffer layer.

The surface magnetic properties of the LSMO layer under varying strain states was investigated using XMCD measurements. These results are shown in Figure 1 and summarized in Table I. With decreasing *c/a* ratio, the magnitude of the Mn XMCD decreases, while the coercive field, *Hc,* increases. For the LSMO layers with intermediate c/a ratio near 0.984, little difference exists in the shape of hysteresis loops taken along the LSMO <100> and <110> pseudocubic directions, in agreement with reports from the literature for LSMO films grown on (001)-oriented STO substrates.[20] In comparison, for films under a small compressive strain or large tensile strain (*c/a* ratio < 0.98), a clear distinction between the two directions is observed, with the easy direction of magnetization lying along the LSMO <110> pseudocubic direction. These XMCD results show that the magnetic properties depend strongly on the strain state of the LSMO film with a sharp decrease in magnetization below a *c/a* ratio of 0.98.
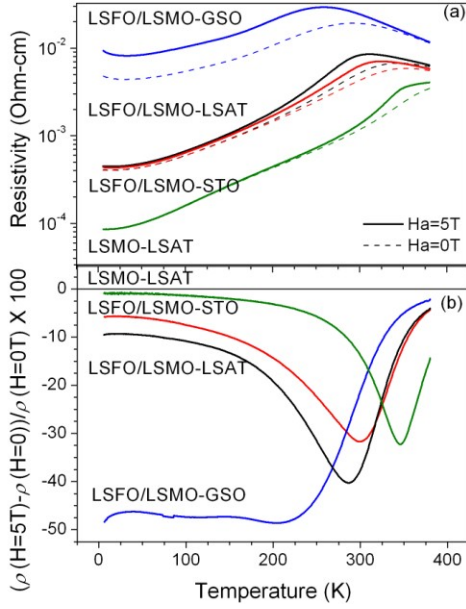
Fig.2. (a) Resistivity measured with *Ha*=0 and 5T and (b) the calculated *MR* as a function of temperature for LSMO layers with varying strain states.
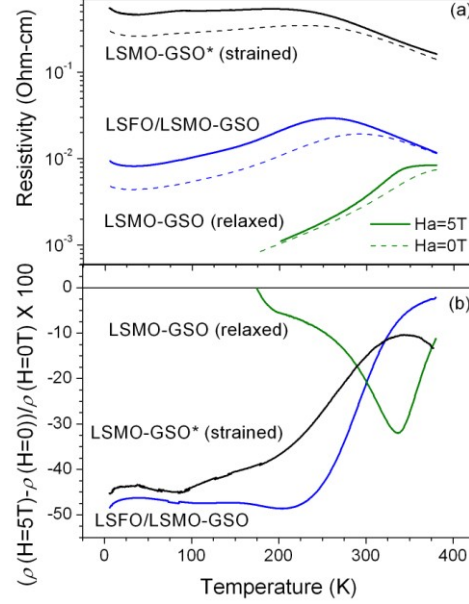

Fig.3. (a) Resistivity measured with *Ha*=0 and 5T and (b) the calculated *MR* as a function of temperature for LSMO layers grown on GSO substrates with varying strain state.

Bulk LSMO displays coincident FM/PM and metal-insulator transitions (MIT) that occur at the T_C[4]. In addition, the magnetoresistance, *MR*, which can be calculated by the equation $MR = \rho\,(H = 5T) - \rho\,(H = 0T) / \rho\,(H = 0T)$, normally shows a peak at the T_C, as at this temperature the disordered Mn spins can easily be aligned by a modest applied magnetic field and thus a marked decrease in resistivity occurs. The magnetotransport properties for LSMO layers with different strain states are shown in Figures 2 and 3. Figure 2 compares LSMO layers grown on different substrates while Figure 3 compares LSMO films grown on GSO substrates using different growth conditions. The resistivity curves for all samples display a MIT with critical temperatures ranging from 200 K and 345 K. As the *c/a* ratio decreases, the resistivity increases, the T_C decreases, and the peak in the *MR* broadens. In general, the samples with a *c/a* ratio > 0.98 show a negative peak in *MR*, which increases in magnitude with decreasing *c/a* ratio. At these strain levels, the MnO_6 octahedral become distorted, both in terms of the Mn-O bond angles and the bond distances, which affects the hopping of electrons along $Mn^{3+} - O^{2-} - Mn^{4+}$ chains. In contrast, for samples with *c/a* ratio < 0.98, the resistivity systematically increases by several orders of magnitude with increasing strain, the MIT broadens significantly, and the *MR* reaches a

plateau value near 50% for temperatures below the T_C instead of showing a peaked shape. Therefore, despite the fact that the LSMO layer displays ferromagnetism, an applied magnetic field is required to impose long-range order on the Mn spins, which results in a decrease in the resistivity. In this regime, the magnetization and resistivity display a strong dependence on the *c/a* ratio, while the *MR* remains nearly unchanged. This behavior may be indicative of the formation of a spin-glass phase or phase separation due to the large tensile strain.[17,21] In fact, using first-principles band structure calculations, Fang *et al.*[22] and Konishi *et al.*[23] predicted that under large tensile strain, LSMO would transition from the FM/metal to the A-type antiferromagnetic (AFM)/insulator state. Close to this boundary one might expect the LSMO layer to phase separate into FM/metal and AFM/insulator regions depending on the local variations in strain state and/or chemical composition. This picture of phase separation is further supported by the reduced magnetization observed in these samples, though further measurements are required to concretely determine the presence of phase separation.

The resistivity and *MR* curves of the partially relaxed LSMO layer on GSO substrate returns to similar values to those reported for the bilayer films on STO and LSAT substrates with similar *c/a* ratio. This result suggests that the

presence of any misfit dislocations as the LSMO layer relaxes has minimal impact on the magnetotransport properties. However, it should be noted that the bilayer films have suppressed T_C ~285-295K. This behavior may arise due to Fe/Mn cation mixing or charge transfer at the LSFO/LSMO interface which has been shown to decrease the T_C of LSMO.[24,25]

In conclusion, this work investigated the effect of epitaxial strain on the magnetic and magnetotransport properties of LSMO thin films. The tetragonal distortion can be tuned continuously from a slight compressive strain of 1.005 to a large tensile strain of 0.952 by choosing the type of substrate, by using an LSFO buffer layer and/or by varying growth rate. As the c/a ratio decreases, the Curie temperature and saturation magnetization decrease monotonically, while the magnetoresistance and the coercive field increase slowly. For c/a ratio > 0.98, these trends are likely due to the distortion of the MnO_6 octahedral which affects the hopping of electrons along $Mn^{3+} - O^{2-} - Mn^{4+}$ chains. For c/a ratio < 0.98 the resistivity quickly increases by several orders of magnitude, the magnetization decreases, and the magnetoresistance reaches a plateau value at low temperatures. In this regime, this behavior may be explained by a phase separation into ferromagnetic/metal and antiferromagnetic/ insulator regions.

[1]E. Dagotto, Science **309**, 257 (2005).
[2]J.H. Park, E. Vescovo, H.J. Kim, C. Kwon, R. Ramesh, T. Venkatesan, Nature **392**, 794 (1998).
[3]M. Bowen, M. Bibes, A. Barthelemy, J.P. Contour, A. Anane, Y. Lemaitre, A. Fert, Appl. Phys. Lett. **82**, 233 (2003).
[4]A.P. Ramirez, J. Phys.: Condens. Matter **9**, 8171 (1997).
[5]Y. Tomioka, A. Asamitsu, H. Kuwahara, Y. Moritomo, Y. Tokura, Phys. Rev. B **53**, 1689 (1996).
[6]P. G. de Gennes, Phys. Rev. **118**, 141 (1960).
[7]J. B. Goodenough, Phys. Rev. **100**, 564 (1955).
[8]H. Y. Hwang, T. T. M. Palstra, S.-W. Cheong, and B. Batlogg, Phys. Rev.B **52**, 15046 (1995).
[9]J. F. Mitchell, D. N. Argyriou, C. D. Potter, D. G. Hinks, J. D. Jorgensen, and S. D. Bader, Phys. Rev. B **54**, 6172 (1996).
[10]Y. Moritomo, A. Asamitsu, and Y. Tokura, Phys. Rev. B **51**, 16491 (1995).
[11]A. Urushibara, Y. Moritomo, T. Arima, A. Asamitsu, G. Kido, and Y.Tokura, Phys. Rev. B **51**, 14103 (1995).
[12]C. Kwon, M. C. Robson, K. -C. Kim, J. Y. Gu, S. E. Lofland, S. M. Bhagat, Z. Trajanovic, M. Rajeswari, T. Venkatesan, A. R. Kratz, R. D. Gomez, R. Ramesh, J. Magn. Magn. Mater. **172**, 229 (1997).
[13]A. Tebano, A. Orsini, D. Di Castro, P. G. Medaglia, and G. Balestrino, Appl. Phys. Lett. **96**, 092505 (2010).
[14]Rajesh V. Chopdekar, Elke Arenholz, and Y. Suzuki, Phys. Rev. B **79**, 104417 (2009).
[15]Y. Takamura, R. V. Chopdekar, E. Arenholz, and Y. Suzuki, Appl. Phys. Lett. **92**, 162804 (2008).
[16]C. Thiele, K. Dörr, O. Bilani, J. Rödel, and L. Schultz, Phys. Rev. B **75**, 054408 (2007).
[17]I. C. Infante, F. Sanchez, J. Fontcuberta, M. Wojcik, E. Jedryka, S. Estrade, F. Peiro, J. Arbiol, V. Laukhin and J. P. Espinos, Phys. Rev. B **76**, 224415 (2007).
[18]V.G. Sathe, S. K. Paranjpe, V. Sirrguri, and A. V. Pimpale, J. Phys.: Condens. Matter **10**, 4045 (1998).
[19]E. Arenholz and S. O. Prestemon, Rev. Sci. Instrum. **76**, 083908 (2005).
[20]L. M. Berndt, V. Balbarin and Y. Suzuki, Appl. Phys. Lett. **77**, 2903 (2000).
[21]Y. Tokura, Rep. Prog. Phys. **69**, 797 (2006).
[22]Z. Fang, I.V. Solovyev, and K. Terakura, Phys. Rev. Lett. **84**, 3169 (2000).
[23]Y. Konishi, Z. Fang, M. Izumi, T. Manako, M. Kasai, H. Kuwahara, M.Kawasaki, K. Terakura, and Y. Tokura, J. Phys. Soc. Jpn. **68**, 3790 (1999).
[24]Y. Takamura, F. Yang, N. Kemik, E. Arenholz, M. D. Biegalski and H. M. Christen, Phys. Rev. B **80**, 180417(R) (2009).
[25]K. H. Ahn, X. W. Wu, K. Liu and C. L. Chien, Phys. Rev. B **54**, 15299 (1996)